Progress in Fractional Differentiation and Applications
An International Journal

http://dx.doi.org/10.18576/pfda/060406

Fractional-order PI-PD Control of Real-time Pressure Process

Kishore Bingi[1,*], *Rosdiazli Ibrahim*[2], *Mohd Noh Karsiti*[2] *and Sabo Miya Hassan*[3]

[1]Department of Control & Automation, School of Electrical Engineering, VIT University, 632014 Vellore, Tamil Nadu, India
[2]Department of Electrical and Electronic Engineering, Universiti Teknologi PETRONAS, 32610 Seri Iskandar, Malaysia
[3]Department of Electrical and Electronics Engineering, Abubakar Tafawa Balewa University, P.M.B. 0248 Bauchi, Nigeria

Received: 2 Sep. 2019, Revised: 20 Oct. 2019, Accepted: 27 Dec. 2019
Published online: 1 Oct. 2020

Abstract: PID controllers are the most widely used because of its advantages of simple design and implementation. However, the controllers produce high overshoot at the initial stage and experience derivative kick effects during the set-point change. On the other hand, the pressure process is highly nonlinear such that its control with PID without modification will be problematic. Therefore, to mitigate these issues this work proposes fractional-ordering of PI-PD controller for the control of the pressure process. The controller retains the simplicity of the PID and maintains the same number of parameters of fractional-order PID. The experimental results show that the proposed controller has performed outperformed PID, PI-PD, and fractional-order PID in terms of overshoot and settling times and disturbance rejection. Furthermore, the controller produces a smoother control signal and reduces the effect of the proportional and derivative kick effects.

Keywords: Pressure process, PI-PD Controller, PID, set-point weighting, fractional-ordering, real-time control.

1 Introduction

The traditional PID controllers are extensively used for the control of process plants in the industry. This is mainly due to its advantages of simple design and tuning and easy real-time implementation [1–5]. However, the PID has the problems of two kick effects namely proportional and derivative which produces high peak-overshoot during the variation in reference signal [6–13]. Therefore, in order to mitigate these kick effects, researchers have developed set-point weighted PID (SWPID) controller [7, 14, 15]. However, this kind of control strategy has six tuning parameters to the three parameters of the conventional PID controller. Thus, to avoid such a scenario, researchers have proposed PI-PD controllers that have the same three tuning parameters as of conventional conventional and at the same time, the control strategy can reduce both the kick effects and peak-overshoots during the change in the reference signal.

Recently, investigating on improving the performance of the controller has been done by various researchers. For example, in [6], [16] and [17], the authors concentrated on structural implementation of the PI-PD controller. In a related development, authors of [18], [19], [2], [20] and [21] implemented the Smith predictor based structure for the process control. Another approach adopted by authors for automatic generation control in [22] and [23] is the cascaded PI-PD which was implemented on power systems. However, an entirely different approach to implementing the PI-PD controller was adopted in [24]. Here, the controller is implemented using the fuzzy logic approach.

The use of fractional-ordering to improve the performance of PID controllers has been discussed by researchers in [7, 25–30]. This is because the controllers provide more flexibility to adjust the dynamic characteristics of the system and less sensitive to parameters changes. In line with this, authors in [26] and [31] proposed a cascaded fractional-order PI-PD controller for level control in coupled two-tank system. The experimental results of coupled thank in the paper shows that the controller outperformed the PI-PD controller in terms of fixed and variable set-point tracking and load disturbance rejection. However, the presented cascaded control is complex compared to a single-loop control as it requires the addition of both measurement and controller.

The contribution of this paper is to propose a fractional-order PI-PD controller for the control of the real-time pressure process using single-loop control. The parameters of the controller will be tuned experimentally using Ziegler-Nichols (ZN) and set-point tracking methods. Furthermore, two single-loop configurations were proposed for the implementation

* Corresponding author e-mail: kishore9860@gmail.com

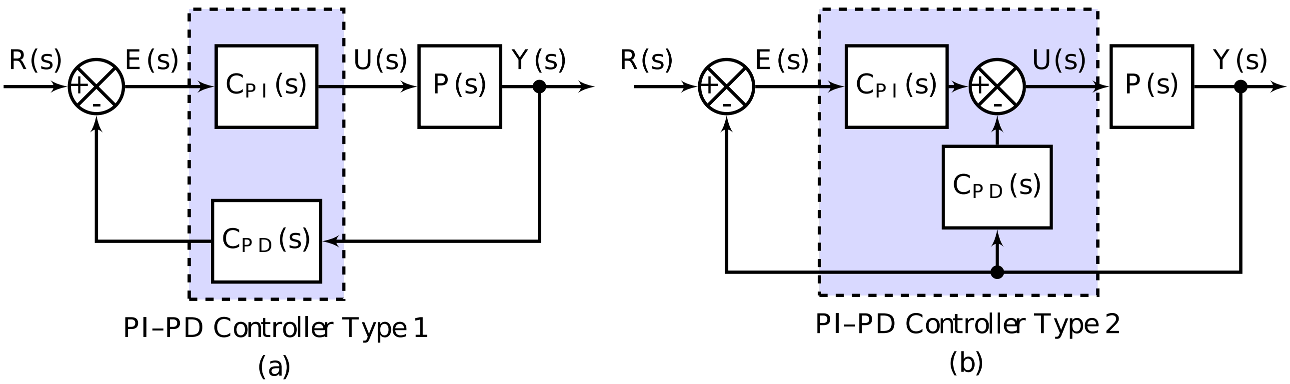

Fig. 1: Single-loop control configurations of PI-PD controller (a) Configuration 1 (b) Configuration 2.

of the proposed controller. The performance of the proposed controller will be evaluated through comparison with PI-PD controllers.

The remaining part of the paper is organized as follows. The design of a fractional-order PI-PD control strategy is given in Section 2. The schematics of the complete experimental set-up is given in Section 3. The results and discussion are presented in Section 4. Finally, conclusions are given in Section 5.

2 Design of fractional-order PI-PD (PI$^\lambda$–PD$^\mu$) controller

For the parallel structure of PID controller with gains K_p, K_i and K_d, the $(U(s))$ is defined as follows:

$$U(s) = \left(K_p + \frac{K_i}{s} + K_d s\right) E(s). \tag{1}$$

From the above equation, $(E(s))$ is defined as $E(s) = R(s) - Y(s)$. Thus, the control signal with respect to $R(s)$ and $Y(s)$ can be written as

$$U(s) = \left(K_p + \frac{K_i}{s} + K_d s\right) R(s) - \left(K_p + \frac{K_i}{s} + K_d s\right) Y(s). \tag{2}$$

From Eq. (2), the $U(s)$ of a SWPID can be derived by weighting the proportional action of first term with $b \in (0,1)$ and derivative action with $c \in (0,1)$ as follows:

$$U(s) = \left(bK_p + \frac{K_i}{s} + cK_d s\right) R(s) - \left(K_p + \frac{K_i}{s} + K_d s\right) Y(s). \tag{3}$$

However, c is set to zero for completely avoiding derivative kick effect in the control action. Thus, Eq. (3) is transformed as follows:

$$U(s) = \left(bK_p + \frac{K_i}{s}\right) R(s) - \left(K_p + \frac{K_i}{s} + K_d s\right) Y(s). \tag{4}$$

Therefore, the fractional-order form of the SWPID controller i.e., SWPI$^\lambda$D$^\mu$ as reported in [7] with fractional parameters $\lambda \in (0,1)$ and $\mu \in (0,1)$ as follows:

$$U(s) = \left(bK_p + \frac{K_i}{s^\lambda}\right) R(s) - \left(K_p + \frac{K_i}{s^\lambda} + K_d s^\mu\right) Y(s). \tag{5}$$

Similarly, from Eq. (1), the control signal of fractional-order PID (PI$^\lambda$D$^\mu$) controller with fractional parameters λ and μ as follows:

$$U(s) = \left(K_p + \frac{K_i}{s^\lambda} + K_d s^\mu\right) E(s). \tag{6}$$

Table 1: Controller configurations derived from PI$^{\lambda}$–PD$^{\mu}$.

Controller Category	Controller Type	λ	μ
PI-PD	P-P	0	0
	P-PD	0	1
	PI-P	1	0
	PI-PD	1	1
PI$^{\lambda}$-PD$^{\mu}$	PI$^{\lambda}$-P	0< λ <1	0
	PI$^{\lambda}$-PD	0< λ <1	1
	P-PD$^{\mu}$	0	0< μ <1
	PI-PD$^{\mu}$	1	0< μ <1
	PI$^{\lambda}$-PD$^{\mu}$	0< λ <1	0< μ <1

Consider the PI and PD transfer functions of the controller with gains k_p, k_i and k_d as follows:

$$C_{PI}(s) = k_p + \frac{k_i}{s}; \;\; C_{PD}(s) = 1 + k_d s. \tag{7}$$

From Eq. (7), to achieve zero steady state error, the gain of the controller kept at one. Furthermore, the implementation of the controller in two configurations is presented in Fig. 1. From the first configuration, the $U(s)$ is obtained as

$$U(s) = \; C_{PI}(s)E(s) = \; C_{PI}(s)\big[R(s) - C_{PD}(s)Y(s)\big]. \tag{8}$$

Thus, by substituting Eq. (7) in (8), we get

$$U(s) = \left(k_p + \frac{k_i}{s}\right)\Big[R(s) - \big(1 + k_d s\big)Y(s)\Big], \tag{9}$$

$$U(s) = \left(k_p + \frac{k_i}{s}\right)R(s) - \left((k_p + k_i k_d) + \frac{k_i}{s} + k_p k_d s\right)Y(s). \tag{10}$$

Furthermore, from the second configuration, the $U(s)$ is given as:

$$U(s) = C_{PI}(s)\big[R(s) - Y(s)\big] - C_{PD}(s)Y(s). \tag{11}$$

After substituting Eq. (7) in (11), we get

$$\begin{aligned} U(s) &= \left(k_p + \frac{k_i}{s}\right)\big[R(s) - Y(s)\big] - \big(1 + k_d s\big)Y(s) \\ &= \left(k_p + \frac{k_i}{s}\right)R(s) - \left((k_p + 1) + \frac{k_i}{s} + k_d s\right)Y(s), \end{aligned} \tag{12}$$

The transfer functions of PI$^{\lambda}$ and PD$^{\mu}$ controllers with fractional parameters λ and μ of PI$^{\lambda}$-PD$^{\mu}$ are as follows

$$C_{PI^{\lambda}}(s) = k_p + \frac{k_i}{s^{\lambda}}, \; C_{PD^{\mu}}(s) = 1 + k_d s^{\mu}. \tag{13}$$

Therefore, the control signal of first configuration based on Eq. (10) is given as

$$U(s) = \left(k_p + \frac{k_i}{s^{\lambda}}\right)R(s) - \left((k_p + k_i k_d) + \frac{k_i}{s^{\lambda}} + k_p k_d s^{\mu}\right)Y(s), \tag{14}$$

Similarly, the control signal of configuration 2 based on Eq. (12) is given in Eq. (15).

$$U(s) = \left(k_p + \frac{k_i}{s^{\lambda}}\right)R(s) - \left((k_p + 1) + \frac{k_i}{s^{\lambda}} + k_d s^{\mu}\right)Y(s). \tag{15}$$

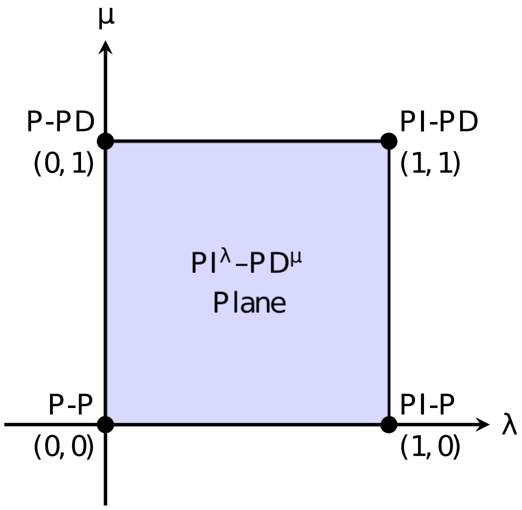

Fig. 2: Graphical representation of various controller configurations on a λ–μ plane.

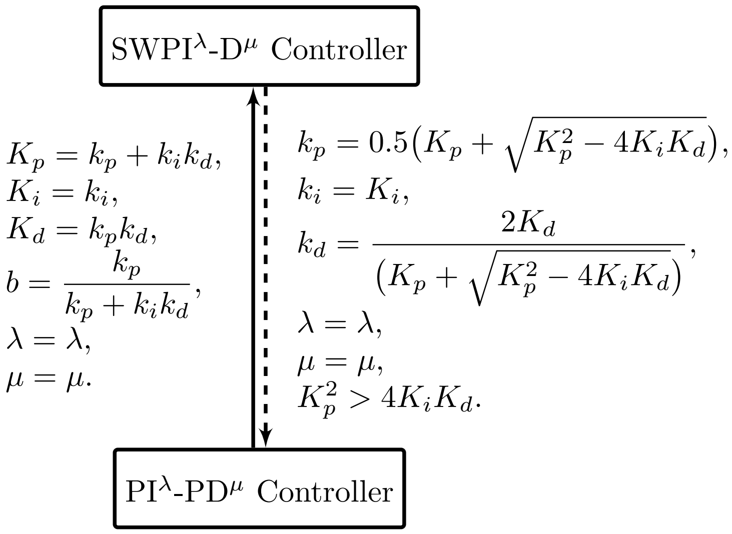

Fig. 3: Conversion of controller parameters

Furthermore, Table 1 gives the integral and differentiator gains of PID controller family derived from the proposed controller. The representation on fractional-order parameter axis of these controllers is shown in Fig. 2. The conversion relations shown in Fig. 3 to convert the SWPI$^\lambda$D$^\mu$ to PI$^\lambda$–PD$^\mu$ will be obtained from Eq. (14). Here, the conversion from SWPI$^\lambda$-D$^\mu$ to PI$^\lambda$-PD$^\mu$ is only possible if $K_p^2 > 4K_iK_d$.

$$U(s) = \left(\left(\frac{k_p}{k_p + k_i k_d}\right)(k_p + k_i k_d) + \frac{k_i}{s^\lambda}\right)R(s) - \left((k_p + k_i k_d) + \frac{k_i}{s^\lambda} + k_p k_d s^\mu\right)Y(s), \tag{16}$$

3 Experimental set-up of real-time pressure process

The experimental set-up of the pressure process is shown in Fig. 4 while Fig. 5 gives the schematics of the set-up. The process consists of a buffer tank VL202 and a pressure transmitter PT202 which is accessed through a peripheral

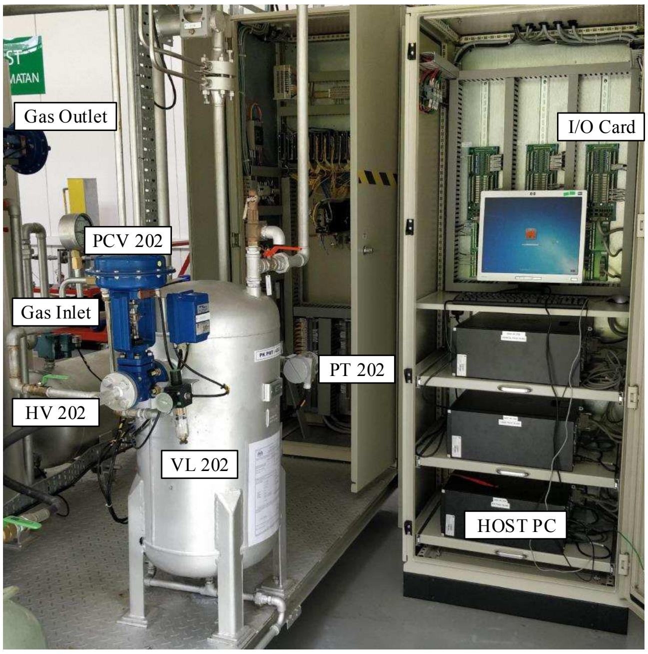

Fig. 4: Experimental set-up of real-time pressure process plant.

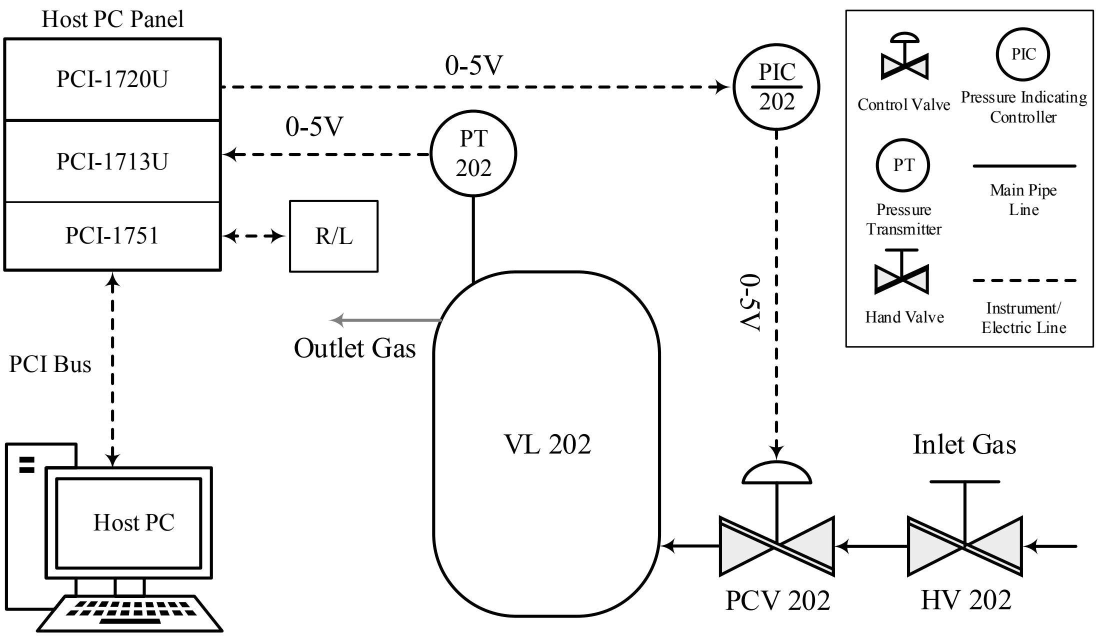

Fig. 5: Schematics of the complete experimental diagram.

component interconnect (PCI) card PCI-1731U; 32-channel analog input card at the host panel. The input gas into the tank is controlled using a pressure control valve PCV202. The signal to the valve is sent through pressure indicating controller PIC202 which is accessed through the PCI-1720U; 4-channel D/A output card. On the other hand, the characteristics of the PCV202 given in Fig. 6 shows that the behavior is nonlinear increasing sensitivity type. To engage the plant either locally or remotely (R/L), a switch is connected to a 48bit digital I/O card i.e., PCI-1751 at the host panel. The host panel is connected to host computer via PCI cables where the proposed controllers will be implemented in MATLAB/SIMULINK.

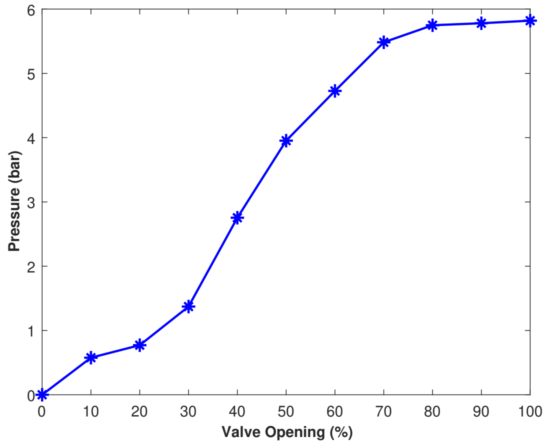

Fig. 6: Characteristics of PCV 202.

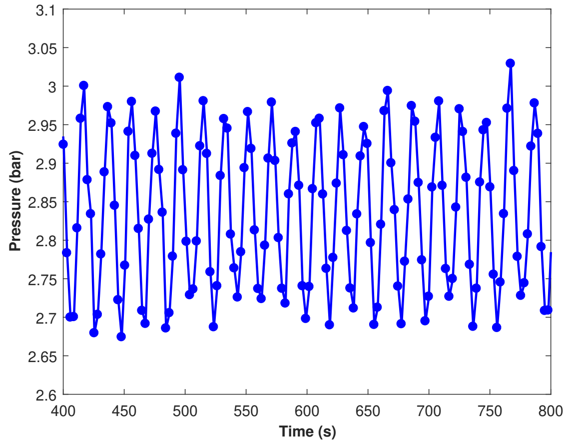

Fig. 7: Uniformed oscillatory behavior of PT202 for ZN tuning.

Table 2: Controller parameters.

Controller	P	I	D	λ	μ
PID	30.0	3.0	1.0	–	–
PI-PD	29.8997	3.0	0.0334	–	–
PI^{λ}–PD^{μ}	29.8997	3.0	0.0334	0.95	0.5

4 Results and discussions

This section presents the performance of PI-PD, fractional PI-PD, and comparison of PI-PD and fractional PI-PD. In all the cases, the performance comparison is done in terms of step-response characteristics and integral performance criteria. The step response characteristics include rise-time, settling time, and overshoot while the performance indices chosen here are integral of absolute error (IAE) and integral of squared error (ISE) are defined as follows:

$$IAE = \int_0^T |e(t)|dt; \;\; ISE = \int_0^T e(t)^2 dt. \tag{17}$$

The oscillatory behavior of pressure transmitter 202 for $K_u = 51$ and $P_u = 20$ is shown in Fig. 7. Therefore, the controller parameters using ZN tuning correlations are given in Table 2. Furthermore, the parameters of the PI-PD controller are obtained based on the conversion relations.

On the other hand, the parameters λ and μ are designed using closed-loop set-point tracking approach. Thus, the effect of variation of controller gains λ and μ on the plant performance are given in Figs. 8 and 9 respectively while Table 3 gives the step-response characteristics of this effect. From Fig. 8, as λ value decreases from one the steady-state error (e_{ss}) increases but reduces in %OS. Furthermore, from the table, it can also be noted that the minimum steady state value of λ is 0.8. Thus, lower than this value of λ will leads to high e_{ss}. Similarly, from Fig. 9, as μ decreases from unity, the performance of the system improves. Furthermore, the oscillations in the control signal also decrease. Thus, the chosen optimal values are $\lambda = 0.95$ and $\mu = 0.5$ as reported in Table 2.

4.1 Performance of conventional controller

The performance with conventional controllers is presented in Fig. 10. The zoomed regions of interest (ROI) is given in Fig. 11 while the characteristics are given in Table 4. From the performance, the reference signal tracking ability of PI-PD configuration 1 controller is performed better compared to PID and configuration 2 of PI-PD. Furthermore, it can be observed from the control signals is that the configuration 1 PI-PD control signal has smoother performance compared to both PID and configuration 2 of PI-PD. This can be seen more clearly in regions C and D of Fig. 13.

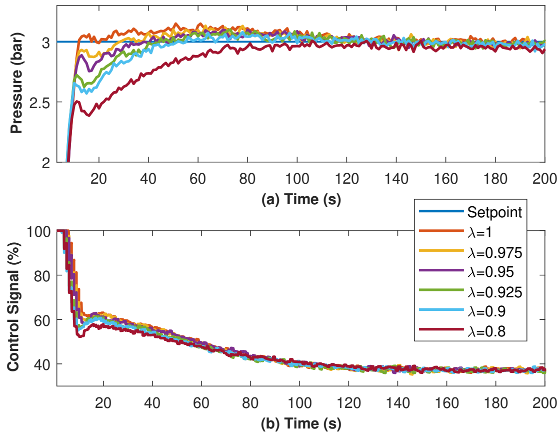

Fig. 8: Plant performance over variation in λ.

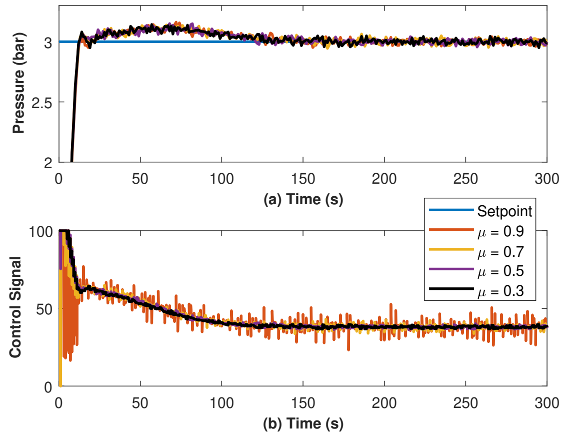

Fig. 9: Plant performance over variation in μ.

Table 3: Steady-state characteristic of plant over variation in λ and μ.

Parameter	Value	t_r	t_s	%OS
λ	1	6.4911	95.3112	5.0151
	0.975	6.6421	77.9867	4.4215
	0.95	6.6913	79.5911	3.2994
	0.925	6.9599	72.2900	3.4077
	0.9	17.8056	70.0560	2.6667
	0.8	32.7617	198.1350	0.2777
μ	0.9	7.0383	88.4318	5.4255
	0.7	7.1283	99.3004	5.0350
	0.5	6.9372	93.6639	4.6373
	0.3	6.7716	85.7019	4.7881

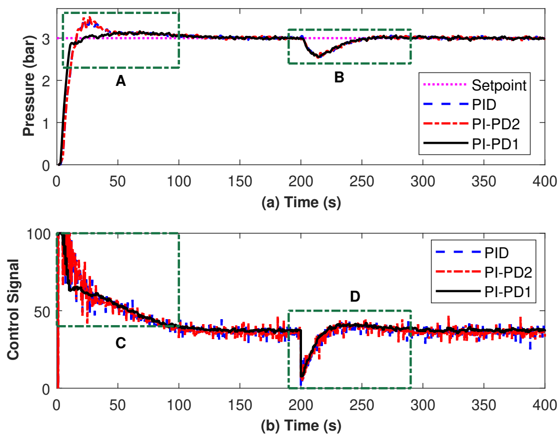

Fig. 10: Performance of real-time pressure process for PI-PD controllers.

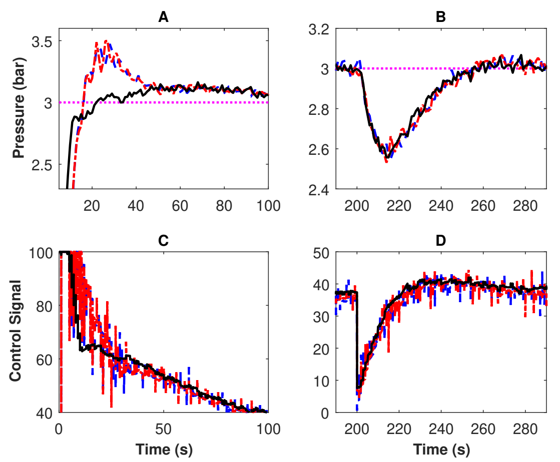

Fig. 11: ROI of Fig. 10.

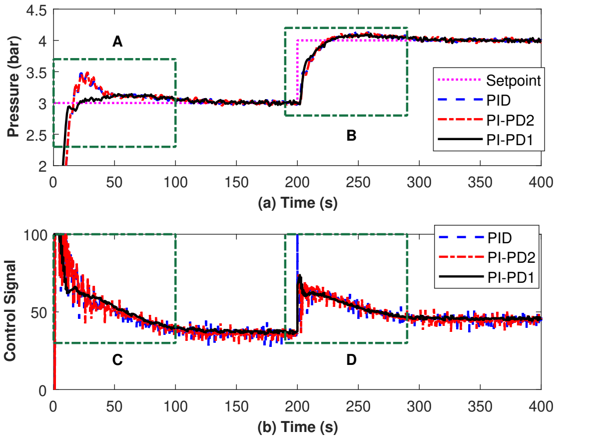

Fig. 12: Performance of real-time pressure process for change in reference signal.

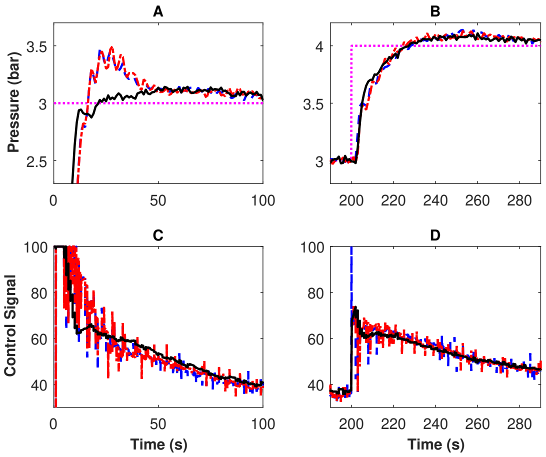

Fig. 13: ROI of Fig. 12.

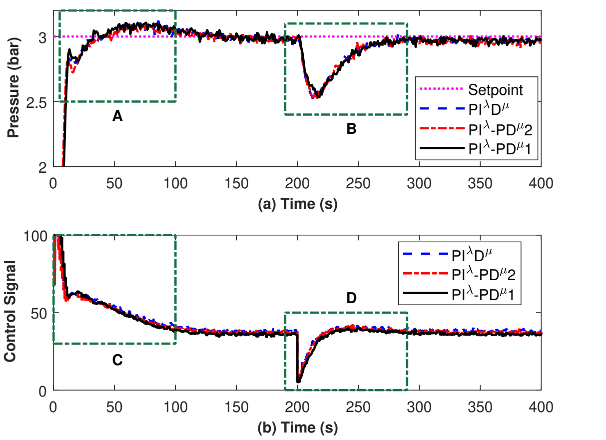

Fig. 14: Performance of real-time pressure process for fractional PI-PD.

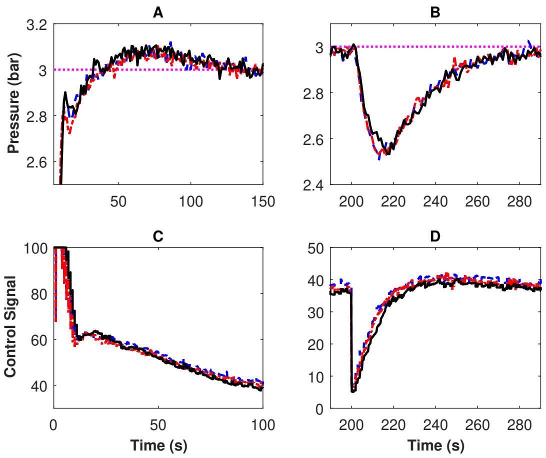

Fig. 15: ROI of Fig. 14.

On the other hand, the performance for variation in reference and RIO of the performance is given in Figs. 12 and 13 respectively. It can be noted from the figures is that the proposed configurations of PI-PD controllers are free from kick effects. This can be seen very clearly in region D of Fig. 13.

4.2 Performance of fractional controllers

The performance comparison for proposed controllers and the ROI of the performance is shown in Figs. 14 and 15 respectively and the numerical characteristics are given in Table 4.

From the performance, it can be observed that the two configurations of the proposed controller performed better that of fractional PID controller with an overshoot of around 3.5% while that of the fractional PID is 4.0737%. Furthermore, the controllers has fastest rise time of 6.6s compared to 7.17s of fractional PID.

Furthermore, the performance for change in reference input and the RIO of the performance is shown in Figs. 16 and 17 respectively. From the figures, during change in reference input, there is a derivative kick effect in the fractional PID has while there is no effects in both of the configurations of fractional PI-PD controllers.

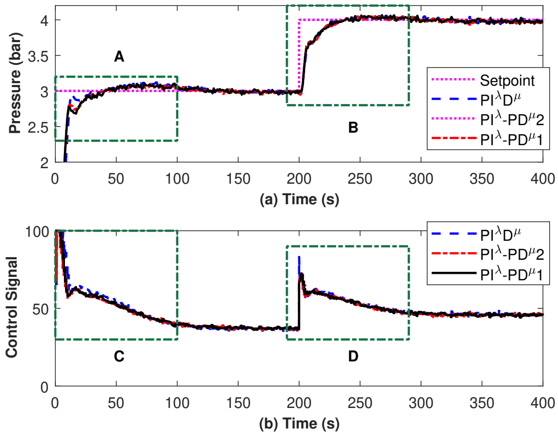

Fig. 16: Performance of real-time pressure process for change in reference signal.

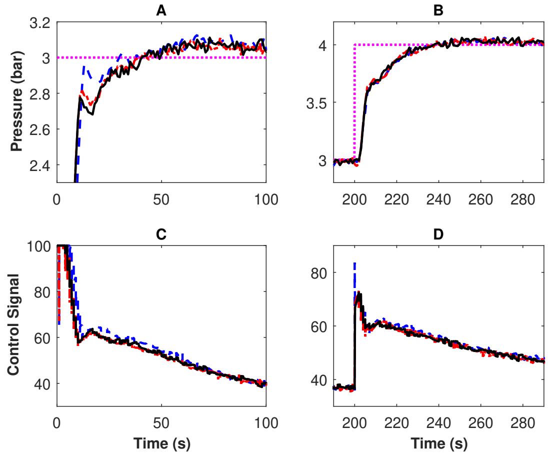

Fig. 17: ROI of Fig. 16.

Table 4: Performance analysis of various PI-PD controllers.

Category	Controller	t_r	t_{s_1}	t_{s_2}	%OS	IAE	ISE
Integer-order Controllers	PID	7.7953	103.9629	240.9393	15.7821	0.1305	0.1396
	PI-PD2	8.0101	105.0095	239.8613	16.6024	0.1318	0.1384
	PI-PD1	6.6580	91.7818	239.3725	5.4441	0.0971	0.0945
Fractional-order Controllers	PI$^\lambda$D$^\mu$	7.1764	86.5618	260.1200	4.0737	0.1085	0.1007
	PI$^\lambda$–PD$^\mu$2	6.6958	78.1124	256.1254	3.5257	0.1059	0.0956
	PI$^\lambda$–PD$^\mu$1	6.6820	86.1941	252.2575	3.5303	0.1134	0.1128

4.3 Performance comparison of both integer-order and fractional-order controllers

The performance of both the configurations of controllers with ROI is given in Figs. 18 and 19 respectively while the characteristics of the performance are given in Table 4. From the configurations 1 controllers, the proposed controller performed better compared to the conventional PI-PD with the least 3.5303% of %OS and fastest 86.1941s of setting time. The disturbance rejection of both conventional and fractional controllers are similar and satisfactory.

On the other hand, from the configuration 2 controllers, the proposed fractional controller performed much better when compared to conventional controller with %OS of 3.5257% and fastest settling and rise times of 78.1124 and 6.6958s respectively. Furthermore, the proposed controller produced smoother control action.

The responses of with both configurations of controllers for change in reference input with RIO of performance is respectively given in Figs. 20 and 21. Furthermore, both the configurations of proposed controllers produced smoother control action and free from kick effects.

5 Conclusion

This paper has proposed fractional-ordering of PI-PD controllers for the control of the pressure process. The implementation of proposed controllers in two single-loop configurations namely configuration 1 and 2 is presented. Furthermore, the conversion relations were developed to convert PID parameters to PI-PD. The experimental results on the pressure plant show that configuration 1 PI-PD outperformed the PID and configuration 2 PI-PD in terms of all the parameters. Both configurations of PI-PD controllers are free from kick effect during change in reference signal. Results also show that the performance of bot the configurations by fractional-ordering is significantly improved when compared to other controllers.

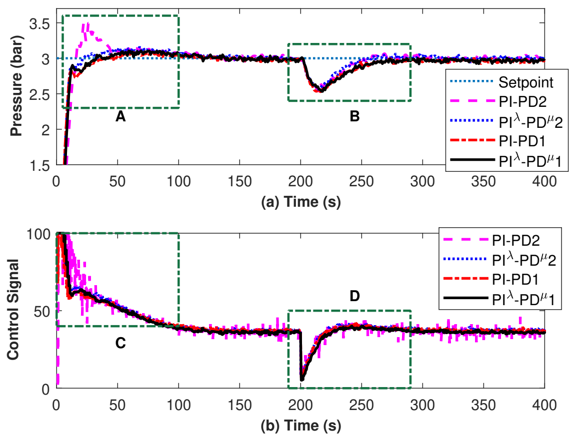

Fig. 18: Performance of real-time pressure process for PI-PD and fractional PI-PD controllers.

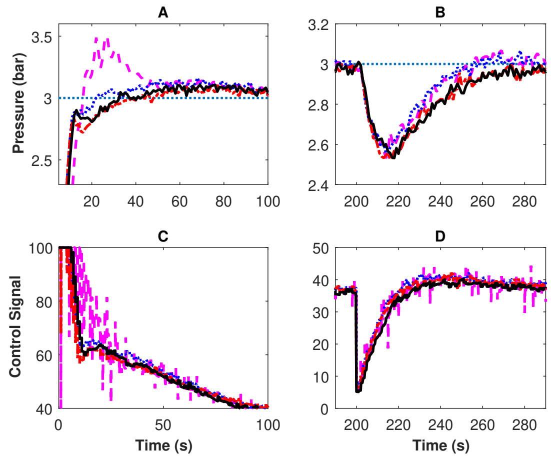

Fig. 19: ROI of Fig. 18.

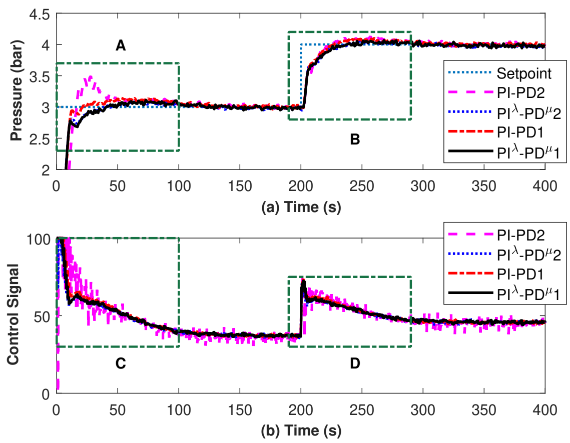

Fig. 20: Performance comparison of real-time pressure process for change in reference signal.

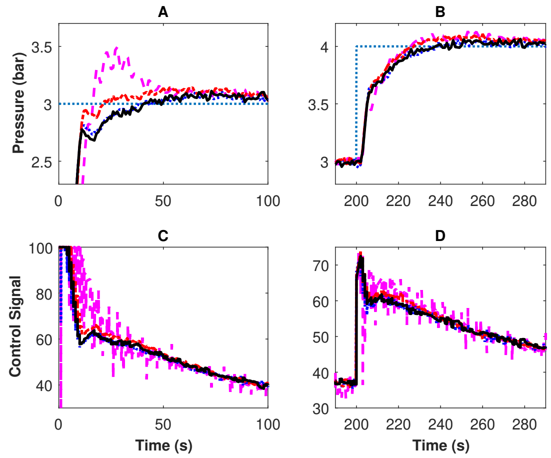

Fig. 21: ROI of Fig. 20.

Acknowledgement

The authors acknowledge the support of YUTP Grants 015LC0-053 and 0153AA-H16.

References

[1] N. Kanagaraj, P. Sivashanmugam and S. Paramasivam, A fuzzy logic based supervisory hierarchical control scheme for real time pressure control, *Int. J. Autom. Comp.* **6**(1), 88–96 (2009).
[2] I. Kaya, PI-PD controllers for controlling stable processes with inverse response and dead time, *Electr. Eng.* **98**(1), 55–65 (2016).
[3] N. Kanagaraj, P. Sivashanmugam and S. Paramasivam, Fuzzy logic based supervisory control scheme for real-time pressure regulation, *Contr. Int. Syst.* **37**(3), 160 (2009).
[4] P. K. Medarametla and M. Muthukumarasamy, A novel PID controller with second order lead/lag filter for stable and unstable first order process with time delay, *Chem. Prod. Proc. Mod.* **13**(1), 1–16 (2018).

[5] K. Bingi, R. Ibrahim, M. N. Karsiti, S. M. Hassan and V. R. Harindran, A comparative study of 2DOF PID and2DOF fractional order PID controllerson a class of unstable systems, *Arch. Contr. Sci.* **28**(4), 635–682 (2018).
[6] K. J. Åström, *Control system design lecture notes for me 155a*, Department of Mechanical and Environmental Engineering University of California Santa Barbara, 2002.
[7] K. Bingi, R. Ibrahim, M. N. Karsiti and S. M. Hassan, Fractional Order Set-point Weighted PID Controller for pH Neutralization Process Using Accelerated PSO Algorithm, *Arab. J. Sci. Eng.* **43**(6), 2687–2701 (2018).
[8] K. Bingi, R. Ibrahim, M. N. Karsiti, S. M. Hassan and V. R. Harindran, Real-time control of pressure plant using 2dof fractional-order pid controller, *Arab. J. Sci. Eng.* **44**(3), 2091–2102 (2019).
[9] K. Johan Åström and T. Hägglund. The future of PID control, *Contr. Engin. Pract.* **9**(11), 1163–1175 (2001).
[10] V. M. Alfaro and R. Vilanova, *Conversion formulae and performance capabilities of two-degree-of-freedom PID control algorithms*, In 17th Conference on Emerging Technologies & Factory Automation (ETFA), 1–6, IEEE, 2012.
[11] M. Araki and H. Taguchi, Two-degree-of-freedom PID controllers, *Int. J. Contr. Automat. Syst.* **1**, 401–411 (2003).
[12] K. H. Ang, G. Chong and Y. Li, PID control system analysis, design, and technology, *IEEE Transact. Contr. Syst. Techn.* **13**(4), 559–576 (2005).
[13] V. M. Alfaro and R. Vilanova, *Model-reference robust tuning of PID controllers*, Springer, 2016.
[14] V. M. Alfaro and R. Vilanova, Model-reference robust tuning of 2DoF PI controllers for first-and secondorder plus dead-time controlled processes, *J. Proc. Contr.* **22**(2), 359–374 (2012).
[15] K. Bingi, R. Ibrahim, M. N. Karsiti, S. M. Hassan and V. R. Harindran, *Fractional Order PI Controllers for Real-time Control of Pressure Plant*. In 2018 5th International Conference on Control, Decision and Information Technologies (CoDIT), 972–977, IEEE, 2018.
[16] K. I. Tsai and C. C. Tsai, *Design and experimental evaluation of robust PID and PI-PD temperature controllers for oil-cooling machines*, In 9th World Congress on Intelligent Control and Automation (WCICA), 535–540, IEEE, 2011.
[17] H. Zou and H. Li, Improved PI-PD control design using predictive functional optimization for temperature model of a fluidized catalytic cracking unit, *ISA Transact.* **67**, 215–221 (2017).
[18] I. Kaya, A PI-PD controller design for control of unstable and integrating processes, *ISA Transact.* **42**(1), 111–121 (2003).
[19] I. Kaya, Obtaining controller parameters for a new PI-PD Smith predictor using autotuning, *J. Proc. Contr.* **13**(5), 465–472 (2003).
[20] S. Nema and P. K. Padhy, Identification and cuckoo PI-PD controller design for stable and unstable processes, *Transact. Inst. Measur. Contr.* **37**(6), 708–720 (2015).
[21] P. K. Padhy and S. Majhi, Relay based PI–PD design for stable and unstable FOPDT processes, *Comput. Chem. Eng.* **30**(5), 790–796 (2006).
[22] S. Padhy and S. Panda, A hybrid stochastic fractal search and pattern search technique based cascade PI-PD controller for automatic generation control of multi-source power systems in presence of plug in electric vehicles, *CAAI Transact. Intel. Tech.* **2**(1), 12–25 (2017).
[23] S. Padhy, S. Panda and S. Mahapatra, A modified GWO technique based cascade PI-PD controller for AGC of power systems in presence of plug in electric vehicles, *Int. J. Eng. Sci. Tech.* **20**(2), 427–442 (2017).
[24] M. P. V. S. Majhi and C. Mahanta, *Fuzzy proportional integral-proportional derivative (PI-PD) controller*, In Proceedings of the 2004 American Control Conference, 5, 4028–4033, IEEE, 2004.
[25] R. Aparecido Aguiar, I. Carlos Franco, F. Leonardi and F. Lima, Fractional PID controller applied to a chemical plant with level and pH control, *Chem. Prod. Proc. Mod.* **13**(4), 1–12 (2018).
[26] B. Kar and P. Roy, A comparative study between cascaded fopi–fopd and iopi–iopd controllers applied to a level control problem in a coupled tank system, *J. Contr. Autom. Electr. Syst.* **29**(3), 340–349 (2018).
[27] C. A. Monje, Y. Q. Chen, B. M. Vinagre, D. Xue and V. Feliu-Batlle, *Fractional-order systems and controls: fundamentals and applications*, Springer, 2010.
[28] P. Shah and S. Agashe, Review of fractional PID controller, *Mechatronics* **38**, 29–41 (2016).
[29] S. K. Verma, S. Yadav and S. K. Nagar, Optimization of fractional order PID controller using grey wolf optimizer, *J. Contr. Autom. Electr. Syst.* **28**(3), 314–322 (2017).
[30] H. S. Ahn, V. Bhambhani and Y. Q Chen, Fractional-order integral and derivative controller for temperature profile tracking, *Sadhana*, **34**(5), 833–850 (2009).
[31] P. Roy, B. Kar and B. K. Roy, Fractional order PI-PD control of liquid level in coupled two tank system and its experimental validation, *Asian J. Contr.* **19**(5), 1–11 (2017).